Mon. Not. R. astr. Soc. (1980) **193**, 439–449

A model for the magnetic-field structure in extended radio sources

R. A. Laing*
Mullard Radio Astronomy Observatory, Cavendish Laboratory, Madingley Road, Cambridge CB3 0HE

Received 1980 March 29; in original form 1980 March 20

Summary. This paper describes a model for the magnetic-field configuration in extended radio sources in which an initially random field has been compressed or sheared to lie entirely in one plane. The polarization properties of radiation from electrons in such a field are evaluated and the expected degree and direction for some simple geometries are derived. The predictions of the model are in good agreement with observations of extragalactic radio sources and of the filaments in the Crab Nebula.

1 Introduction

Synchrotron radiation from extended radio sources is often highly polarized, and this has usually been taken to indicate uniformity of the magnetic fields within them. It is the purpose of this paper to point out that a high degree of polarization does not necessarily imply that the field is uniform; for example it could be confined to a plane containing the line-of-sight. Högbom (1979) has argued that magnetic fields in extragalactic radio sources are basically irregular, but that shear and/or compression will make them anisotropic, thus producing regions of high polarization. Simple field configurations based on the compression of an initially random field are discussed quantitatively in this paper. The analysis was motivated by the observation that the degree of polarization in extragalactic radio sources often approaches its theoretical maximum value at the edges of a source, where the apparent field is aligned with the boundary, but drops to a minimum in the centre of the structure (e.g. Burch 1979a; Högbom 1979). A natural explanation is that an irregular field has been compressed so as to be tangential to the boundaries of the source; the degree of polarization is then highest when the line-of-sight is parallel to the plane of compression (i.e. at the edge).

The polarization properties of a slab of field, initially random in direction, which has been compressed in one dimension are evaluated in Section 2 (mathematical details being relegated to the Appendix) and applications to jets in extragalactic radio sources are outlined. Field configurations appropriate to the filaments of the Crab Nebula and to the extended

* Present address: National Radio Astronomy Observatory, Edgemont Road, Charlottesville, Virginia 22901, USA.

emitting regions of extragalactic radio sources are discussed in Sections 3 and 4 respectively. A brief summary is given in Section 5.

Throughout this paper, the effects of Faraday rotation and depolarization will be ignored and the radiating regions will be assumed to be optically thin; the apparent magnetic field direction is then perpendicular to the E-vector of linearly-polarized radiation.

2 The polarization properties of radiation from a region of compressed magnetic field

2.1 THE MODEL

The field configuration of this model is that obtained by the anisotropic compression of a volume containing a randomly-orientated field. As a specific example, consider a cube containing a field which is disordered on a scale much smaller than its dimensions and which is compressed parallel to one of its axes (Fig. 1). The field is then effectively confined to one plane, but its direction within that plane is still random on a scale small compared with the beamwidth of observation. The aim of this section is to evaluate the degree of polarization expected from a uniform and isotropic distribution of radiating electrons in such a field when the plane of the slab makes an arbitrary angle, β, with the line-of-sight.

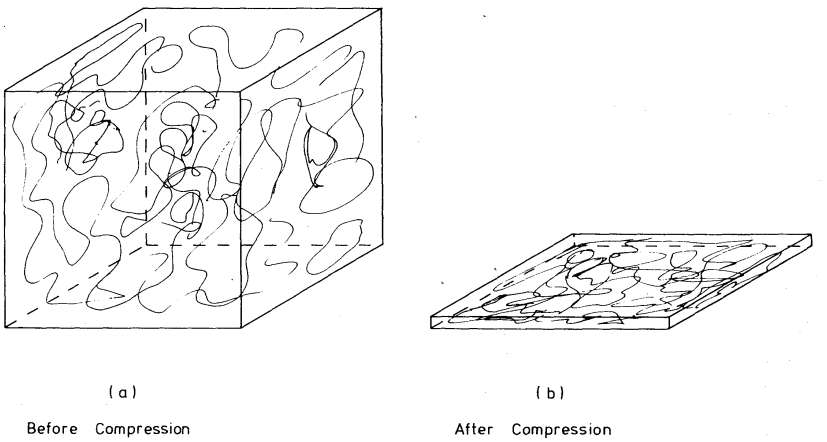

Figure 1. The compression of a cube containing an initially random magnetic field.

Suppose that there is an energy distribution of radiating electrons

$$N(E)\,dE = KE^{-(2\alpha+1)}\,dE,$$

giving rise to synchrotron radiation with spectral index α, defined by $S \propto \nu^{-\alpha}$. The degree of polarization will be a maximum (equal to that for a uniform field) when the slab is edge-on ($\beta = 0$) and zero when it is face-on ($\beta = 90°$). If the slab is orientated so that the E-vector of its polarized radiation is in position angle 0° (see Appendix) then the Stokes parameters $U = 0$ and $Q > 0$.

Since the degree of polarization is independent of the strength of the field, there is no loss of generality in assuming the magnitude of the field to be constant over the slab. The field at any point in the slab is then specified by one angle, θ, the azimuthal angle in the plane of the slab (see Appendix). The Stokes parameters of the radiation from the slab are derived by averaging over θ, all directions being assumed equally probable, so that the flux densities are

$$I = k\int_0^{2\pi} B(\theta)^{\alpha+1}\, d\theta, \tag{1}$$

$$U = kp_{\max}\int_0^{2\pi} B(\theta)^{\alpha+1}\sin 2\chi(\theta)\, d\theta = 0, \tag{2}$$

$$Q = kp_{\max}\int_0^{2\pi} B(\theta)^{\alpha+1}\cos 2\chi(\theta)\, d\theta, \tag{3}$$

where θ is an azimuthal angle in the plane of the slab (see Appendix), $B(\theta)$ is the component of the magnetic field perpendicular to the line-of-sight, $\chi(\theta)$ is the position angle of linearly-polarized radiation from an element of the slab, $p_{\max} = (3\alpha + 3)/(3\alpha + 5)$ is the intrinsic degree of polarization from a region of uniform field (e.g. Pacholczyk 1970), and k is a constant which depends on the number density of radiating electrons and the volume of the slab, but which is irrelevant for the calculation of percentage polarization.

The integrals for I, U and Q are evaluated analytically in the Appendix. A simple solution exists for a spectral index $\alpha = 1$, in which case

$$I = I_0(1 + \sin^2\beta), \tag{4}$$

$$U = 0, \tag{5}$$

$$Q = (3I_0/4)\cos^2\beta, \tag{6}$$

where I_0 is a constant.

2.2 NUMERICAL VALUES

The percentage polarizations expected for values of α in the range 0–2 have been evaluated numerically and are presented in Table 1. The ratio of the degree of polarization, p, to its maximum value $p_{\max}$, is plotted against inclination, β, for $\alpha = 0$, 1 and 2 in Fig. 2. The

Table 1. Percentage polarization for a slab of compressed magnetic field at an inclination β to the line-of-sight.

Spectral index	β/degree									
α	0	10	20	30	40	50	60	70	80	90
0.00	60.00	52.42	40.30	28.77	19.23	11.84	6.45	2.80	0.69	0
0.25	65.22	58.51	46.10	33.41	22.50	13.92	7.59	3.29	0.81	0
0.50	69.23	63.39	51.11	37.61	25.55	15.87	8.67	3.76	0.93	0
0.75	72.41	67.36	55.47	41.46	28.41	17.73	9.71	4.21	1.04	0
1.00	75.00	70.61	59.29	45.00	31.14	19.53	10.71	4.66	1.15	0
1.25	77.14	73.31	62.65	48.28	33.74	21.27	11.70	5.09	1.26	0
1.50	78.95	75.58	65.60	51.31	36.23	22.97	12.67	5.52	1.36	0
1.75	80.49	77.51	68.21	54.12	38.61	24.62	13.61	5.93	1.46	0
2.00	81.82	79.15	70.52	56.73	40.90	26.24	14.55	6.35	1.57	0

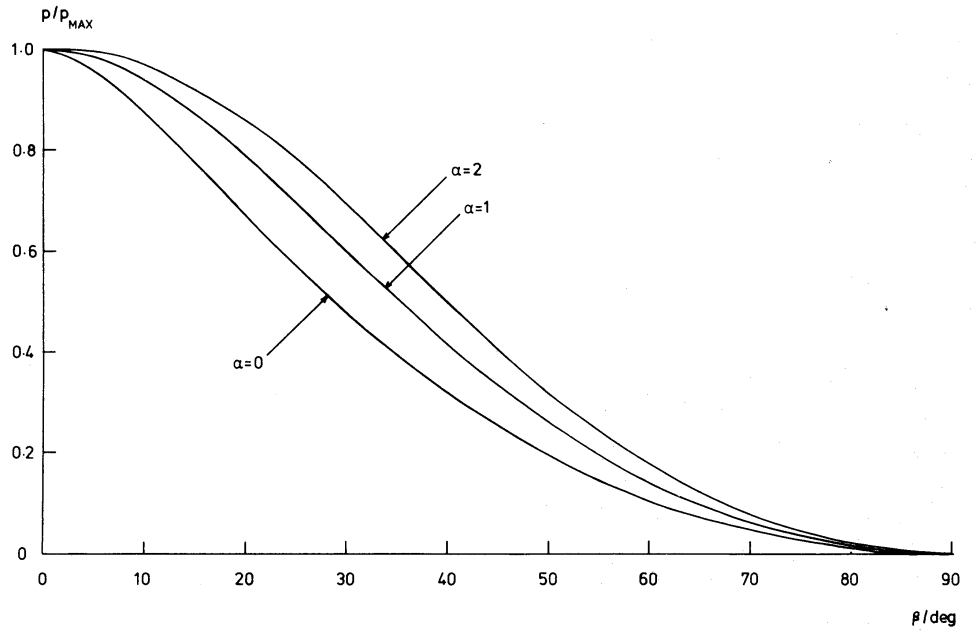

Figure 2. The variation of p/p_{max} with inclination, β, for a slab of compressed field. The values of spectral index are $\alpha = 0$, 1 and 2.

variation of the degree of polarization with β is very similar for different values of α, so that it is justifiable to use the simple solution for $\alpha = 1$

$$p/p_{max} = \cos^2\beta/(1 + \sin^2\beta)$$

as an illustrative example in Section 4.

2.3 JETS IN EXTRAGALACTIC RADIO SOURCES

There are now several extragalactic radio sources which have jets with well-determined field directions (see Laing 1980a, for a list), and in all cases the field is either perpendicular or parallel to the jet axis, although three of the sources have parallel fields close to their nuclei but perpendicular fields further out.

The polarization properties of a jet with an apparent field *perpendicular* to its axis can be described by a model in which the magnetic field has no component along the axis, but is randomly orientated normal to this direction. Such a configuration is expected to develop in a freely-expanding jet containing a tangled field, since if magnetic flux is conserved in a conical expansion and r is the radius of the jet, then the component of B along the jet axis varies as r^{-2} and the perpendicular component as r^{-1}. At sufficiently large distances from the nucleus of the source, the magnetic field is effectively confined to a plane perpendicular to the jet axis, exactly as in the slab model of Section 2.1. The angle between the jet axis and the line-of-sight is then $90° - \beta$ in the notation of that section. The degree of polarization has its maximum possible value when the jet is transverse to the line-of-sight and varies with inclination as given in Table 1; there should be no variation of the degree or direction of polarization across the jet. If such a model applies, it should be possible to place limits on the inclination of a jet to the line-of-sight from measurements of its percentage polarization. High degrees of polarization are expected to be relatively common: for a spectral index of 0.5 (a typical value for the known jets) and a random distribution of orientations, half the sources should have percentage polarizations > 38 per cent (Table 1). Note, however, that simple models of freely-expanding jets are incapable of explaining the variation of surface

brightness with distance from the nucleus (e.g. Burch 1979b); reacceleration of the radiating electrons appears to be required and the effects of this on the field configuration are unknown.

A field configuration which may be appropriate for jets with apparent fields parallel to their axes is discussed in Section 4 (model B).

3 Cylindrical shells: the filaments of the Crab Nebula

Swinbank (1980) has described a model for the radio emission associated with the filaments of the Crab Nebula in which magnetic field and relativistic particles moving away from the central pulsar collide with the slower-moving, dense filaments, thus creating regions of highly-compressed field around them. Here it is assumed that any uniform component of the field within these regions is weak (see Swinbank 1980). Most of the emission is expected to come from the side of the filament nearest to the pulsar, where the field is most highly compressed, so that a suitable idealized model consists of a thin cylindrical layer of magnetic field which is wrapped around *one* side of the filament; this is sketched in Fig. 3. The thickness, r, of the shell is assumed to be negligible compared with the radius, R, of the filament. The field configuration is then that of the slab model discussed in Section 2, but with the orientation, β, changing across the filament. If a filament is inclined at an angle δ to the line-of-sight, the angle between the surface of the shell and the line-of-sight is

$$\beta = \sin^{-1}(\sin\phi \sin\delta), \tag{7}$$

where ϕ is the angle defined in Fig. 3, and $\cos\phi = x/R$.

We consider various orientations of the filament to the line-of-sight, supposing that the resolution of the observations is much less than R.

(a) FILAMENT PERPENDICULAR TO THE LINE-OF-SIGHT

$\delta = 90°$, so that $\beta = \phi$. The percentage polarization reaches its maximum value (65 per cent, corresponding to a spectral index of $\alpha = 0.26$) at the edges of the filament and drops to 0 at its centre; the apparent magnetic field is aligned along the filament.

(b) FILAMENT PARALLEL TO THE LINE-OF-SIGHT

Here, the shell is aligned along the line-of-sight so that the percentage polarization is always 65 per cent; the apparent magnetic field is directed around the filament.

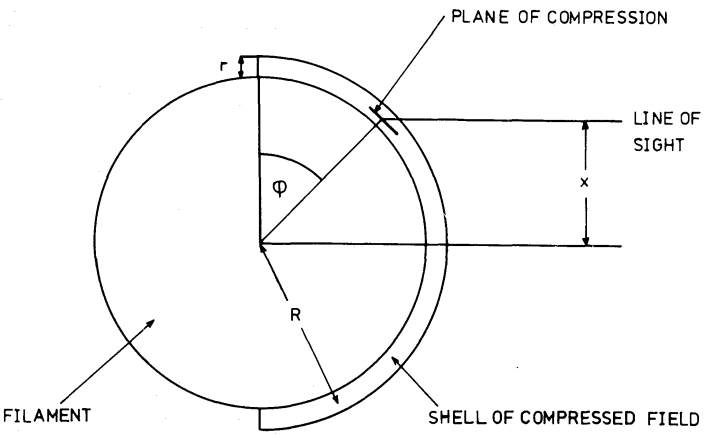

Figure 3. A cross-section perpendicular to the axis of a filament, showing the idealized geometry used in the evaluation of the polarization properties.

(c) FILAMENT AT AN ARBITRARY ANGLE TO THE LINE-OF-SIGHT

For any orientation, δ, the polarization reaches its maximum possible value, p_{max}, at the edges of the filament (where the shell is parallel to the line-of-sight) and drops to a minimum (corresponding to $\beta = \delta$) at the centre. The latter value is non-zero for any value of α unless $\delta = 90°$. The position angle, ζ, of the apparent field at a distance x from the axis of a filament of radius R inclined at an angle δ to the line-of-sight is given by

$$\tan\zeta = -\tan\phi\cos\delta = \frac{-\cos\delta(1-x^2/R^2)^{1/2}}{x/R}.$$

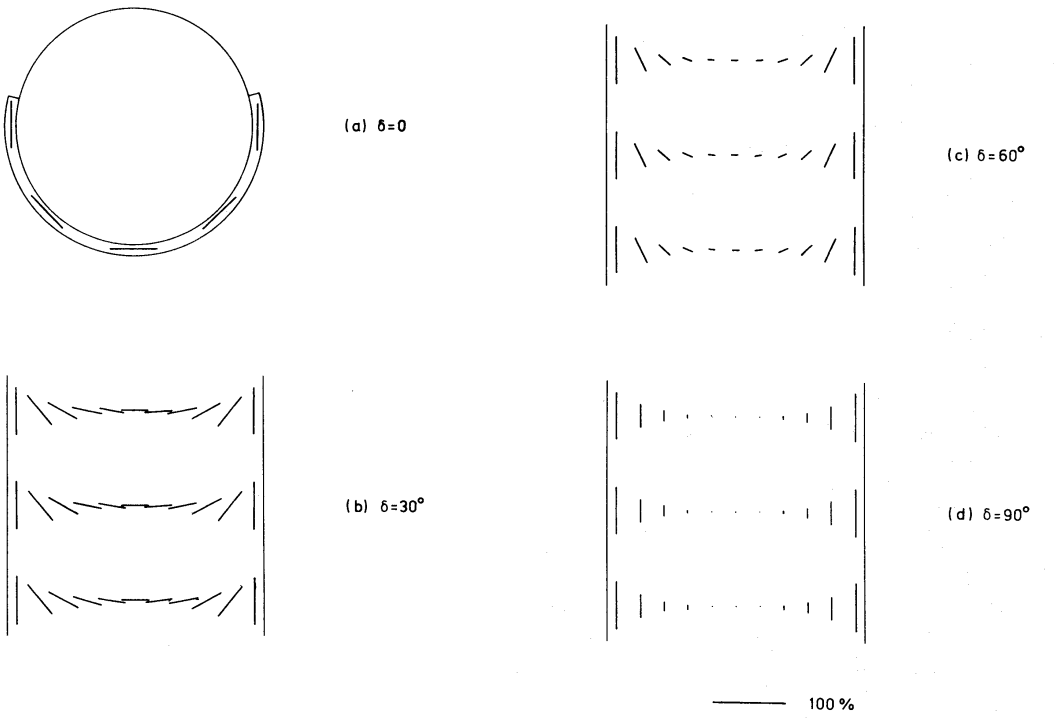

Figure 4. Vector maps of the polarization for filaments with axes inclined at angles δ = 0, 30°, 60° and 90° to the line-of-sight. The lengths of the vectors are proportional to the degree of polarization (the scale is indicated by a horizontal bar), and their directions are those of the apparent magnetic field. A spectral index of 0.26 (appropriate to the Crab Nebula) has been assumed.

The behaviour of the degree of polarization when the inclination of the filament to the line-of-sight is varied can be derived from Table 1 ($\alpha = 0.25$) and equation (7). Vector diagrams showing the magnitude and direction of the polarization for orientations of δ = 0, 30°, 60° and 90° are given in Fig. 4(a)–(d).

The experimental evidence is discussed by Swinbank (1980), who shows that the predictions of the model are in good agreement with observations of the Crab Nebula at 2.7 and 23 GHz.

4 Tangential fields: extragalactic radio sources

The apparent field in extended extragalactic radio sources is almost invariably aligned with the boundaries of the radio emission close to the edges of extended emitting regions, where the percentage polarization has its maximum value. Good examples are presented by Burch (1979a), Forster *et al.* (1978), Högbom (1979), Laing (1980b), Miley, Wellington &

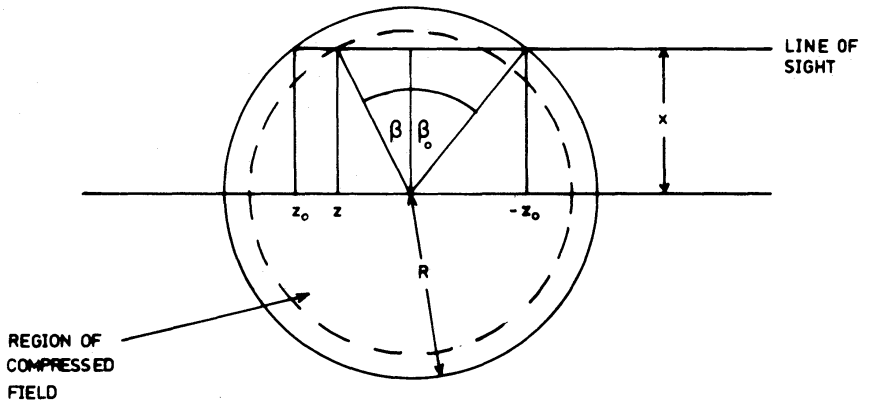

Figure 5. Coordinates used in the calculation of the percentage polarization in a spherical or cylindrical geometry. The diagram shows a cut through the centre of a sphere or perpendicular to the axis of a cylinder; the field (which fills the whole volume) has been sheared so as to be tangential to the boundary, but has no radial component.

van der Laan (1975), Riley (in preparation), Strom, Willis & Wilson (1978), van Breugel (1980a, b) and Willis & Strom (1978). This type of behaviour suggests a class of models in which an initially random field has been sheared so as to be tangential to the boundaries of the structure but has no outward component. Two simple geometries have been considered in order to illustrate the polarization properties of radiation from such a field: a sphere (model A) and a cylinder (model B). In both cases, the emission is taken as coming from the *whole* of the volume rather than being localized in a shell. Emission from a shell would lead to limb-brightening which is unusual, although not unknown (see Laing 1980b). The field is assumed to be randomly orientated within a shell of given radius, but to have no radial component.

The geometry for the calculation of the degree of polarization is shown in Fig. 5, in which the cylinder is assumed to be perpendicular to the line-of-sight. For a line-of-sight at a distance x from the centre of the sphere (or the axis of the cylinder), and a spectral index of $\alpha = 1$ (a typical value for extended extragalactic radio sources which is also computationally convenient), the total and polarized flux densities are I and P respectively, where, from equations (4)–(6)

$$I = k\int_{-z_0}^{z_0} (1 + \sin^2\beta)\, dz = kx(4\tan\beta_0 - 2\beta_0),$$

$$P = \frac{3k}{4}\int_{-z_0}^{z_0} \cos^2\beta\, dz = kx\,\frac{3\beta_0}{2},$$

where $\beta_0 = \cos^{-1}(x/R)$. The degree of polarization is

$$p = \frac{3\beta_0}{4(2\tan\beta_0 - \beta_0)}.$$

As expected, the degree of polarization reaches its maximum possible value at the edges, where the plane of compression is parallel to the line-of-sight and drops to zero in the middle. Vector maps of the apparent field are given in Fig. 6(a) and (b) for models A and B respectively. A combination of the two geometries (a cylinder with hemispherical end-caps; model C) is illustrated in Fig. 6(c).

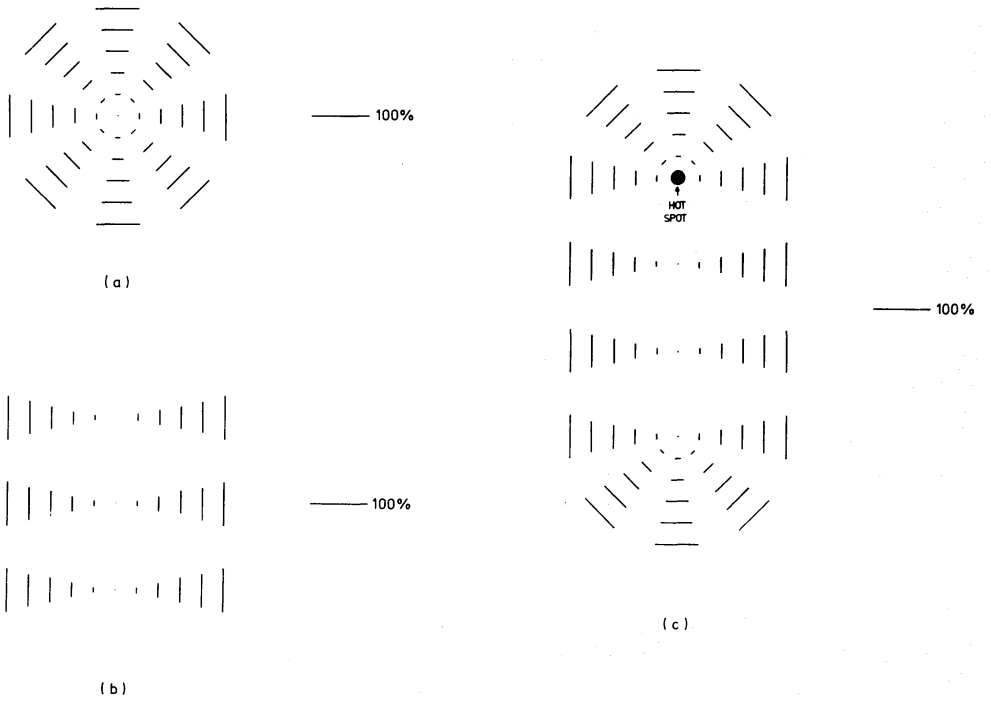

Figure 6. Vector maps of the polarization for the three field configurations discussed in Section 4. The lengths of the vectors are proportional to the percentage polarization (the scale is indicated by a horizontal bar) and the directions are those of the projected magnetic field: (a) a sphere, (b) a cylinder, (c) a cylinder with hemispherical end-caps. As discussed in the text, this model applies to powerful double radio sources and the expected position of the hot-spot in the radio lobe is marked.

Model A provides a good description of the polarization properties of the diffuse outer lobes found in weak radio galaxies (e.g. 3C 272.1; Riley, in preparation), whereas model B may apply to the long streamers of emission found in the sources classified by Simon (1978) as bent-double or twin-tail (e.g. 3C 465; van Breugel 1980b), and also to jets in which the apparent fields are parallel to the axes (e.g. M 87; Laing 1980a). Powerful sources with hot-spots can be described by model C (a number of examples are given by Burch 1979b, Högbom 1979 and Laing 1980b).

5 Summary

The main purpose of this paper has been to point out that the high percentage polarizations observed in extended radio sources do not necessarily imply that the magnetic fields are uniform, but merely that they are confined to planes containing the line-of-sight. Models based on the compression or shearing of an initially random field have been devised to account for the polarization properties of the filaments of the Crab Nebula and of a wide variety of extragalactic radio sources. Features common to most of these models are that the degree of polarization rises towards the edges of an emitting region and that the apparent field direction is tangential to the boundary.

The models are deliberate oversimplifications; in particular, the following effects are ignored:

(a) The angle θ (Section 2.1) is assumed to be randomly distributed. This is unlikely to be true in the case of anisotropic compression (e.g. in jets).

(b) The velocities of the radiating electrons are taken to be uniform and anisotropic. The assumption of uniformity does not hold in an irregular field and the distribution of directions is unlikely to remain isotropic under anisotropic compression.

The derived degrees and directions of linear polarization are in excellent qualitative agreement with observation, but further work is needed: to test the quantitative predictions of the models, using high-resolution observations, to establish how the field configurations could be formed in extragalactic radio sources and to take account of the oversimplifications discussed above.

Acknowledgments

I am grateful to Peter Scheuer, John Shakeshaft, Elizabeth Swinbank and an anonymous referee for helpful advice, and acknowledge financial support from the SRC and the Cavendish Laboratory.

References

Burch, S. F., 1979a. *Mon. Not. R. astr. Soc.*, **186**, 519.
Burch, S. F., 1979b. *Mon. Not. R. astr. Soc.*, **187**, 187.
Forster, J. R., Dreher, J., Wright, M. C. H. & Welch, W. J., 1978. *Astrophys. J.*, **221**, L3.
Högbom, J. A., 1979. *Astr. Astrophys. Suppl.*, **36**, 173.
Laing, R. A., 1980a. *Mon. Not. R. astr. Soc.*, **193**, 427.
Laing, R. A., 1980b. *Mon. Not. R. astr. Soc.*, in press.
Miley, G. K., Wellington, K. J. & van der Laan, H., 1975. *Astr. Astrophys.*, **38**, 381.
Pacholczyk, A. G., 1970. *Radio Astrophysics*, W. H. Freeman & Co., San Francisco.
Simon, A. J. B., 1978. *Mon. Not. R. astr. Soc.*, **184**, 537.
Spain, B. & Smith, M. G., 1970. *Functions of Mathematical Physics*, van Nostrand Reinhold, London.
Strom, R. G., Willis, A. G. & Wilson, A. S., 1978. *Astr. Astrophys.*, **68**, 367.
Swinbank, E., 1980. *Mon. Not. R. astr. Soc.*, **193**, 451.
van Breugel, W. J. M., 1980a. *Astr. Astrophys.*, **81**, 265.
van Breugel, W. J. M., 1980b. *Astr. Astrophys.*, in press.
Willis, A. G. & Strom, R. G., 1978. *Astr. Astrophys.*, **62**, 375.

Appendix: Analytical solution for the polarization of radiation from a compressed field

A1 INTRODUCTION

Coordinates are defined as follows:

β is the angle between the plane of the slab and the line-of-sight;

x, y, z are rectangular coordinates with the z-axis pointing towards the observer and the y-axis parallel to the plane of the slab (Fig. A1);

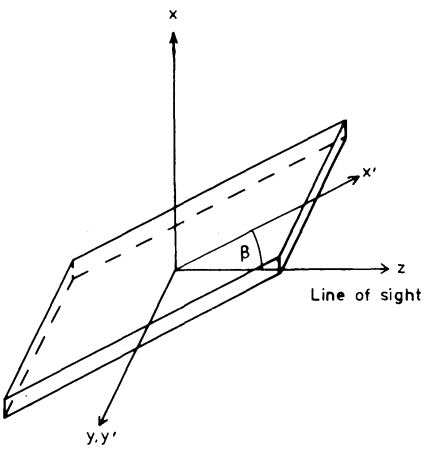

Figure A1. Coordinates used in the calculation of the polarization properties of a slab of compressed field.

x', y' are coordinates in the plane of the slab, y' is parallel to y;

θ is the angle between the field direction and the x' axis at any point in the slab; and

χ is the position angle of the E-vector of the polarized radiation, measured from the x-axis in the x–y plane (i.e. the plane perpendicular to the line-of-sight).

Then for a point in the slab

$x = x' \sin\beta,$

$y = y',$

$z = x' \cos\beta.$

The magnetic-field vector at a point in the slab is

$\mathbf{B} = (B_x, B_y, B_z) = B(\cos\theta \sin\beta, \sin\theta, \cos\theta \cos\beta)$

so that

$B_\perp = B(\cos^2\theta \sin^2\beta + \sin^2\theta)^{1/2}$

$$\tan\chi = -\frac{\sin\beta}{\tan\theta},$$

and hence

$$\cos 2\chi = -\frac{\sin^2\beta - \tan^2\theta}{\sin^2\beta + \tan^2\theta}, \qquad \sin 2\chi = -\frac{2\tan\theta \sin\beta}{\sin^2\beta + \tan^2\theta}.$$

The field directions are uniformly distributed between 0 and 2π, so that equations (1)–(3) give:

$$I = C\int_0^{2\pi} d\theta\,(\cos^2\theta \sin^2\beta + \sin^2\theta)^{(\alpha+1)/2} \tag{A1}$$

$$U = -C\left(\frac{3\alpha+3}{3\alpha+5}\right)\int_0^{2\pi} d\theta(\cos^2\theta \sin^2\beta + \sin^2\theta)^{(\alpha-1)/2} \sin 2\theta \sin\beta = 0$$

$$Q = -C\left(\frac{3\alpha+3}{3\alpha+5}\right)\int_0^{2\pi} d\theta(\cos^2\theta \sin^2\beta + \sin^2\theta)^{(\alpha-1)/2}(\cos^2\theta \sin^2\beta - \sin^2\theta) \tag{A2}$$

(C is a constant).

A2 EVALUATION OF THE INTEGRALS FOR I AND Q

The integrals in equations (A1) and (A2) are simply related to the Laplace integrals for the Legendre and Associated Legendre functions (e.g. Spain & Smith 1970, pp. 136–138)

$$P_q(z) = \frac{1}{\pi}\int_0^{\pi} [z + \cos x(z^2-1)^{1/2}]^q dx$$

$$P_q^m(z) = \frac{(q+1)(q+2)\ldots(q+m)}{\pi}\int_0^{\pi} [z + \cos x(z^2-1)^{1/2}]^q \cos mx\, dx$$

$P_q(z)$ is the Legendre function of order q,

$P_q^m(z)$ is the Associated Legendre function of degree m and order q.

With the aid of the substitutions

$$z = \frac{1 + \sin^2\beta}{2\sin\beta} \quad \text{and} \quad x = 2\theta,$$

equations (A1) and (A2) can be reduced to

$$I = 2\pi C(\sin\beta)^{(\alpha+1)/2} P_{(\alpha+1)/2}\left[\frac{1 + \sin^2\beta}{2\sin\beta}\right] \tag{A3}$$

and

$$Q = \pi C\left(\frac{3\alpha + 3}{3\alpha + 5}\right)(\sin\beta)^{(\alpha-1)/2}\left[\frac{2(1 + \sin^2\beta)}{\alpha + 1} P^1_{(\alpha-1)/2}\left(\frac{1 + \sin^2\beta}{2\sin\beta}\right)\right.$$

$$\left. + \cos^2\beta\ P_{(\alpha-1)/2}\left(\frac{1 + \sin^2\beta}{2\sin\beta}\right)\right]. \tag{A4}$$

There is a simple solution when $\alpha = 1$, in which case equations (A1) and (A2) reduce to

$$I = C\int_0^{2\pi} d\theta(\cos^2\theta\ \sin^2\beta + \sin^2\theta) = \pi C(1 + \sin^2\beta),$$

$$Q = -\frac{3C}{4}\int_0^{2\pi} d\theta(\cos^2\theta\ \sin^2\beta - \sin^2\theta) = \frac{3\pi C}{4}\cos^2\beta.$$

These results can be obtained from equations (A3) and (A4) by the substitutions $\alpha = 1$, $P_1(z) = z, P_0^1(z) = 0$ and $P_0(z) = 1$.